

## Chapter 2

# Methodology

Courage Kamusoko

**Abstract** Remote sensing, GIS, and land change models (LCMs) are critical for mapping urban land use/cover and simulating “what if” urban growth scenarios, particularly in developing countries experiencing rapid urbanization. The purpose of this chapter is to describe briefly the methodology used to produce land use/cover maps, and simulate land use/cover changes for selected metropolitan areas in Asia and Africa. Land use/cover maps were classified from Landsat imagery for 1990, 2000, 2010, and 2014 using the random forest (RF) classifier. Quantitative accuracy assessment was not conducted for the 1990 land use/cover maps due to lack of reference data. However, qualitative and quantitative accuracy assessment was performed for the 2000, 2010, and 2014 land use/cover maps based on Google Earth imagery. Overall land use/cover classification accuracy for all land use/cover maps ranged from 70 to 90%. Land use/cover changes were simulated based on the boosted regression trees-cellular automata (BRT-CA) and RF-CA LCMs. We evaluated the goodness-of-fit of transition potential maps, and validated the simulated land use/cover changes based on robust statistical measures. Generally, the BRT-CA and RF-CA LCMs for all metropolitan areas in Asia and Africa performed relatively well. In particular, the BRT-CA and RF-CA LCMs for metropolitan areas in Africa had the best performance. The modeling and simulation results presented in this chapter provide an initial exploration of BRT-CA and RF-CA LCMs in Asia and Africa. This chapter demonstrates the significance of robust calibration, validation, and simulation of spatial LCMs for all metropolitan areas in Asia and Africa.

---

C. Kamusoko (✉)  
Asia Air Survey Co., Ltd, Kawasaki, Japan  
e-mail: kamas72@gmail.com

## 2.1 Introduction

The past decades have witnessed tremendous development of land change models (LCMs) due to availability of remote sensing data, advances in geographical information and social sciences as well as theoretical developments of complexity and self-organizing systems (Tobler 1979; Wolfram 1984; Couclelis 1985; Engelen 1988; Batty 1998, 2005; Wu and Webster 1998; Torrens 2008; The State of Land Change Modeling 2014). To date, numerous LCMs have been developed to model and simulate land use/cover changes (Wu and Webster 1998; Verburg et al. 1999; Messina and Walsh 2001; Soares-Filho et al. 2002), deforestation (Lambin 1997; Geoghegan et al. 2001; Mas et al. 2004), urban growth (Couclelis 1989; Clarke et al. 1997; Cheng and Masser 2004; Yeh and Li 2009), climate change (Dale 1997), and hydrology (Matheussen et al. 2000).

While LCMs have highlighted significant insights into landscape change processes, most of these models have been criticized for lacking robust calibration and validation procedures (Pontius and Malanson 2005; Vliet et al. 2011). For example, previous studies show that transition potential maps—which are key inputs of LCM—have been validated using the relative operating characteristic (ROC) area under the curve (AUC) statistic (Eastman et al. 2005). However, the AUC statistic has limitations, especially for validating transition potential maps (Mas et al. 2013; Pontius and Parmentier 2014; Pontius and Si 2014) since it includes persistence areas (Eastman et al. 2005). For example, Kamusoko and Gamba (2015) demonstrated that the AUC can be large due to correctly predicted persistence not correctly predicted change (The State of Land Change Modeling 2014). Furthermore, percent correct and the standard Kappa statistics have been widely used to validate LCM (Verburg et al. 2004, Pontius and Malanson 2005; Vliet et al. 2011). However, the use of standard Kappa statistic for validating LCM has been criticized given its tendency to overestimate the agreement between the simulated and observed (reference) maps (Hagen 2002; Pontius et al. 2002). It has also been noted that the standard Kappa statistic neither reveals the components of agreement and disagreement between the simulated and observed (reference) maps nor accounts for persistence (that is, land use/cover classes that do not change during the simulation) (Pontius et al. 2007, 2008).

More recently, numerous statistical measures for calibrating and validating LCMs have been developed to overcome limitations of the ROC statistic and standard Kappa. For example, Pontius and Si (2014) developed the total operating characteristic (TOC) statistic to validate transition potential maps. The TOC statistic provides information such as misses and correct rejections in addition to ROC statistic such as hits (hits plus misses) and false alarms (false alarms plus correct rejections) (Pontius and Si 2014).

More importantly, the TOC statistic shows the actual units in the contingency table (e.g., square kilometers) instead of a unitless statistic such as AUC (Pontius

and Si (2014). Furthermore, Visser and de Njis (2006) and Vliet et al. (2011) developed additional accuracy assessment statistics, which take into account information contained in the initial land use/cover map and the proportion of persistent land use/cover classes during the simulation period. The KSimulation expresses the agreement between the simulated land use/cover transitions and reference land use/cover transitions, while KTranslocation measures the degree to which the transitions agree in terms of allocations (Vliet et al. 2011). The KTransition captures the agreement in terms of quantity of built-up and non-built-up transitions (Vliet et al. 2011). The KSimulation, KTransition, and KTranslocation statistics are available in the Map Comparison Kit software by Visser and de Njis (2006). Pontius et al. (2007, 2008) also introduced the Figure of Merit (FoM), which expresses agreement between the observed and simulated changes for validating simulated land use/cover changes.

While these novel statistics have provided a new paradigm for validation, to date, few studies (Kamusoko and Gamba 2015) have applied these robust statistical measures for validating LCMs. Therefore, more research is needed to better understand uncertainty of LCMs based on the above-mentioned validation statistics. This is critical since LCMs are being considered as useful procedures or tools to establish business-as-usual baselines for urban growth and other land use/cover change studies (The State of Land Change Modeling 2014; Kamusoko and Gamba 2015). The purpose of this chapter is to describe briefly the methodology used to produce the land use/cover maps, calibrate and validate LCMs (in this case, both transition potential and simulated land use/cover maps). The specific objectives of this chapter are to evaluate the goodness-of-fit of transition potential maps, validate the simulated land use/cover maps, and elucidate components of agreement and disagreement. Validation statistics developed by Pontius and Si (2014), Pontius and Malanson (2005), Visser and de Njis (2006), and Vliet et al. (2011) as well as simple GIS overlay analysis are used in this chapter.

This chapter is organized as follows: Sect. 2.2 provides an overview of the image processing and change analysis; Sect. 2.3 describes land change modeling implementation procedures for all the metropolitan areas in Asia and Africa; Sect. 2.4 presents the results and discussions; while Sect. 2.5 provides the summary and conclusion of the chapter.

## 2.2 Image Processing and Change Analysis

### 2.2.1 *Satellite Imagery and Reference Data*

Landsat 4 and 5 Thematic Mapper (TM), Landsat 7 Enhanced Thematic Mapper Plus (ETM+), and Landsat 8 datasets were used for land use/cover classification

(Tables 2.1 and 2.2). All the Landsat datasets were acquired between 1988 and 2014 (Tables 2.1 and 2.2). The selection of the image data was based on the availability of high-quality satellite imagery with minimal cloud cover. Landsat 8 (originally called Landsat Data Continuity Mission) was launched on February 11, 2013, as the eighth

**Table 2.1** Summary of Landsat imagery used for Metropolitan Areas in Asia

Metropolitan area	Landsat sensor	Path/row	Acquisition date
Bangkok	L4 TM	129/50	30/03/1988
		129/51	30/03/1988
	L7 ETM+	129/50	20/12/1999
		129/51	20/12/1999
	L5 TM	129/50	19/01/2009
		129/51	19/01/2009
Beijing	L4 TM	129/50	17/01/2014
		129/51	17/01/2014
	L7 ETM+	123/32	25/12/1988
		123/33	25/12/1988
	L5 TM	123/32	30/04/2000
		123/33	30/04/2000
Dhaka	L4 TM	123/32	14/03/2009
		123/33	14/03/2009
	L8	123/32	29/04/2014
		123/33	29/04/2014
Hanoi	L4 TM	137/44	13/02/1989
	L7 ETM+	137/44	28/02/2000
	L5 TM	137/44	15/03/2010
	L8	137/44	30/03/2014
Hanoi	L5 TM	127/45	11/09/1988
	L7 ETM+	127/45	20/12/1999
	L5 TM	127/45	05/11/2009
	L8	127/45	19/01/2014
Jakarta	L5 TM	122/64	03/05/1989
	L7 ETM+	122/64	16/08/2001
	L5 TM	122/64	21/05/2010
	L8	122/64	25/08/2013
Kathmandu	L5 TM	141/41	24/01/1989
	L7 ETM+	141/41	04/11/1999
	L5 TM	141/41	11/02/2010
	L8	141/41	26/03/2014
Manila	L5 TM	116/50	02/04/1993
	L7 ETM+	116/50	26/11/2001
	L5 TM	116/50	05/03/2009
	L8	116/50	07/02/2014

(continued)

**Table 2.1** (continued)

Metropolitan area	Landsat sensor	Path/row	Acquisition date
Tehran	L5 TM	164/35	19/09/1988
	L4 TM	165/35	16/09/1987
	L7 ETM+	164/35	18/07/2000
		165/35	25/07/2000
	L5 TM	164/35	22/07/2010
	L8	164/35	08/12/2014
		165/35	13/11/2014
Yangon	L5 TM	132/48	26/02/1989
	L7 ETM+	132/48	21/11/1999
	L5 TM	132/48	24/01/2009
	L8	132/48	23/02/2014

**Table 2.2** Summary of Landsat imagery used for Metropolitan Areas in Africa

Metropolitan area	Sensor	Path/row	Acquisition date
Bamako	L4 TM	199/51	22/03/1990
	L7 ETM+	199/51	30/12/2000
	L5 TM	199/51	16/01/2010
	L8	199/51	16/03/2014
Dakar	L4 TM	205/50	15/10/1989
	L7 ETM+	205/50	04/11/1999
	L5 TM	205/50	25/10/2010
	L8	205/50	17/03/2013
Harare	L5 TM	170/72	23/06/1990
	L7 ETM+	170/72	30/09/2000
	L5 TM	170/72	26/05/2009
	L8	170/72	24/05/2014
Johannesburg	L5 TM	170/78	25/07/1990
	L7 ETM+	170/78	28/07/2000
	L5 TM	170/78	26/05/2009
	L8	170/78	25/06/2014
Lilongwe	L5 TM	168/70	11/07/1990
	L5 TM	168/70	02/06/1999
	L5 TM	168/70	22/08/2011
	L8	168/70	26/07/2013
Nairobi	L5 TM	168/61	17/10/1988
	L7 ETM+	168/61	21/02/2000
	L5 TM	168/61	19/08/2010
	L8	168/61	03/02/2014

satellite in the Landsat program (NASA 2013; USGS 2013). Landsat 8 consists of the Operational Land Imager (OLI) and the Thermal Infrared Sensor (TIRS), which provide images at a spatial resolution of 15 m (panchromatic), 30 m (visible, NIR, SWIR), and 100 m (thermal) (NASA 2013; USGS 2013).

### 2.2.2 *Random Forest Classification*

A modified land cover classification scheme was used for image classification. Three land use/cover classes were considered in this study: (1) built-up; (2) non-built-up; and (3) water. Detailed descriptions of the land use/cover classes are provided in Table 2.3. Land use/cover maps were produced from the classification of Landsat imagery for 1990, 2000, 2010, and 2014 using the (RF) classifier, an ensemble decision tree machine learning method (Breiman 2001). The RF classifier combines bootstrap sampling to construct many individual decision trees, from which a final class assignment is produced (Breiman 2001). This machine learning classifier can be used to learn nonlinear relationships, particularly in heterogeneous urban landscapes. The RF classifier has been demonstrated to be effective for accurate land cover mapping across complex and heterogeneous landscapes (Rodriguez et al. 2012). All the Landsat imagery for all metropolitan areas were classified using the “randomForest” package (Liaw and Wiener 2002), which is available in R (R Development Core Team 2005).

Quantitative accuracy assessment for the 1990 land use/cover maps was not conducted because of the unavailability of reference data such as aerial photographs and high-resolution satellite imagery. However, the Atlas of Urban Expansion developed by the Lincoln Institute of Land Policy (Angel et al. 2010) was used to visually check the quality of land use/cover maps for the 1990 epoch (that is, Landsat imagery acquired between 1988 and 1993). Qualitative and quantitative accuracy assessment was conducted for land use/cover maps from 2000, 2010, and 2014 epochs. The primary reference data for accuracy assessment was obtained from very high-resolution images (e.g., QuickBird image) in Google Earth™

**Table 2.3** Land use/cover classes

Class	Description
Built-up	Residential, commercial and services, industrial, transportation, communication and utilities, construction sites, and landfills
Non-built-up	All wooded areas, riverine vegetation, shrubs and bushes, grass cover, golf courses, parks, cultivated land, fallow land, land under irrigation, bare exposed areas and transitional areas
Water	Rivers, reservoirs, and other water bodies

(Google Earth 2015). Overall land use/cover classification accuracy for all land use/cover maps (from 2000 to 2014) ranged from 70 to 90% for all the metropolitan areas.

2.3 Land Change Modeling

2.3.1 Data

We used land use/cover maps and driving factors to develop spatial LCMs for all metropolitan areas (Table 2.4). Major roads were obtained from OpenStreetMap data, while city center was digitized from Google Earth. Elevation was derived from ASTERGDEM, while population density data were acquired from the LandScan data (Bhaduri et al. 2007). We used built-up areas (extracted from the 1990 and 2010 land cover maps), major roads, and city center data to compute “distance to built-up areas”, “distance to major roads”, and “distance to city center” using the Euclidean distance procedures available in ArcGIS 10.2. We computed “distance to built-up areas” for 1990 and 2010, and “distance to major roads” because built-up areas and roads are dynamic driving factors that change over time. Furthermore, we used “distance to built-up areas” as the driving factor because previous urban form influences future urban patterns (Liu 2009). Finally, all driving factors were resampled to 30 m × 30 m spatial resolution in order to match the spatial resolution of the Landsat-derived land use/cover maps.

2.3.2 Model Calibration and Simulation

We used the following procedures to implement the LCMs for all metropolitan areas: (I) computing transition rates, (II) transition potential modeling, and (III) CA simulation. Machine learning and statistical algorithms available in R were used to model transition potential, while functions available in Dinamica Environment for Geoprocessing Objects (EGO) were used to compute transition rates and simulate land use/cover changes. R is a free and open-source statistical and computer graphic

**Table 2.4** Input data for calibrating and simulating land use/cover change

Variable	Source
Land use/cover maps (1990, 2000, and 2010)	Classified from landsat data
Distance to built-up areas (1990, 2000, 2010)	Derived from land use/cover
Distance to major roads (1990–2000, 2000–2010)	Open street map
Distance to city center	Digitized from Google Earth
Elevation	ASTER GDEM
Population density (2000, 2010)	LandScan data

software (R Core Development Team 2005), while **Dinamica EGO** is a freeware that was developed by Soares-Filho et al. (2009). **Dinamica EGO** consists of a sophisticated platform for developing dynamic spatial models, which involve nested iterations, multiple-step transitions, dynamic feedbacks, and multiscale approaches (Soares-Filho et al. 2009).

#### (I) Computation of transition rates

We used land use/cover maps for 1990, 2000, and 2010 to compute multiple-step transition rates in Dinamica EGO. Multiple-step transition rates refer to transition rates that are computed at annual time step. Therefore, the “1990–2000”, “2000–2010”, and “1990–2010” multiple-step transition rates for all the metropolitan areas were used as input for the final CA simulation run following the methodology described in Kamusoko and Gamba (2015).

#### (II) Computation of transition potential maps

In order to compute the “non-built-up to built-up” transition potential maps, “non-built to built-up” change map from 1990 to 2010, biophysical and socio-economic driving factors were combined based on two machine learning procedures. First, the RF model (Breiman 2001) was used to compute transition potential maps for all metropolitan areas. RF is a machine learning approach, which builds regression trees to describe the relationship between the response and predictor variables (Breiman 2001). In general, multiple trees are built, each based on a bootstrap sample of the data and a random subset of the predictors. The final model predictions are an average prediction across component trees. Previous studies have shown that the RF model is effective for modeling transition potential maps (Kamusoko and Gamba 2015). However, preliminary transition potential calibration results indicated overfitting problems for some metropolitan areas such as Beijing, Bamako, Dhaka, Hanoi, Johannesburg, Kathmandu, and Nairobi. Therefore, an alternative method based on boosted regression trees (BRT) (Friedman 2002; Elith et al. 2008) was employed. BRT is also a machine learning approach, which forms a relationship between a response variable and its predictors without a priori specification of a data model (Friedman 2002; Elith et al. 2008). Generally, a large number of simple models are combined to form a final model (Elith et al. 2008). The main advantage of the BRT model is that it uses a sequential model-fitting algorithm, which reduces both bias and variance and therefore improves model accuracy.

In this study, approximately 2000 training points randomly sampled from “non-built-up to built-up” and “no change” (that is, built-up and non-built-up persistence) areas between 1990 and 2010 were used to fit the BRT and RF models. Generally, 70% of the training areas were used for model development, while 30% were used for cross-validation. The *gbm* and *dismo* packages (Ridgeway 2006; Elith et al. 2008) available in R were used to fit the BRT model. The BRT model



was optimized by changing the learning rate, tree complexity, and number of trees parameters. The learning rate controls the weight that is given to each component tree, while the complexity controls the number of nodes within each tree (Ridgeway 2006; Elith et al. 2008). We set the initial number of trees to five, learning rate to a maximum of 0.001, and bagging fraction to 0.5 (that is, at each iteration 50% of the data is drawn at random, without replacement from the full training set) for each metropolitan area. After many iterations, the best model was selected to compute a “non-built-up to built-up” transition potential map for each metropolitan area.

The RF model was used to compute “non-built-up to built-up” transition potential maps for Bangkok, Jakarta, Manila, Tehran, Yangon, Dakar, Harare, and Lilongwe. The “randomForest” (Liaw and Wiener 2002) package available in R was used to fit the RF model. The RF model parameters were adjusted by changing the number of input variables selected at each node split and the total number of trees included in the model (25, 50, 100, and 500) in order to achieve optimum model performance. After calibration, between 100 and 500 trees were used to construct the final RF model and then compute the “non-built-up to built-up” transition potential maps.

Figures 2.1 and 2.2 show “non-built-up to built-up” transition potential maps for metropolitan areas in Asia and Africa, respectively. Visual analysis revealed that the BRT and RF models produced relatively accurate transition potential maps. In particular, the BRT and RF models were relatively good at modeling built-up areas near previous built-up areas (from 1990 to 2010). In general, the transition potential maps have identified the areas where a change is likely to occur. As a result, the transition potential maps can be used as a useful input to the CA models.

### (III) Cellular automata (CA) simulations

The initial land use/cover map (1990), the transition potential maps (1990–2010), and the three multiple-state transition rates were used to simulate land use/cover up to 2014 based on cellular automata (CA) functions available in Dinamica EGO. The expander transition function expands or contracts previous land use/cover class patches, while the patcher transition function forms new patches (Soares-Filho et al. 2009). The expander and patcher transition functions are composed of an allocation mechanism responsible for identifying cells with the highest transition potential for each transition (Soares-Filho et al. 2009). In order to simulate land use/cover changes, both transition functions use a stochastic selecting mechanism (Soares-Filho et al. 2009). The sizes of new land use/cover patches are set according to a lognormal probability function, whose parameters are defined by the mean patch size (MPS), patch size variance (VAR), and isometry (ISO). The CA model for each metropolitan area was calibrated by changing the parameters of the expander and patcher transition functions using trial and error. The initial simulation year was set to 1990, while the final year was set to 2014.

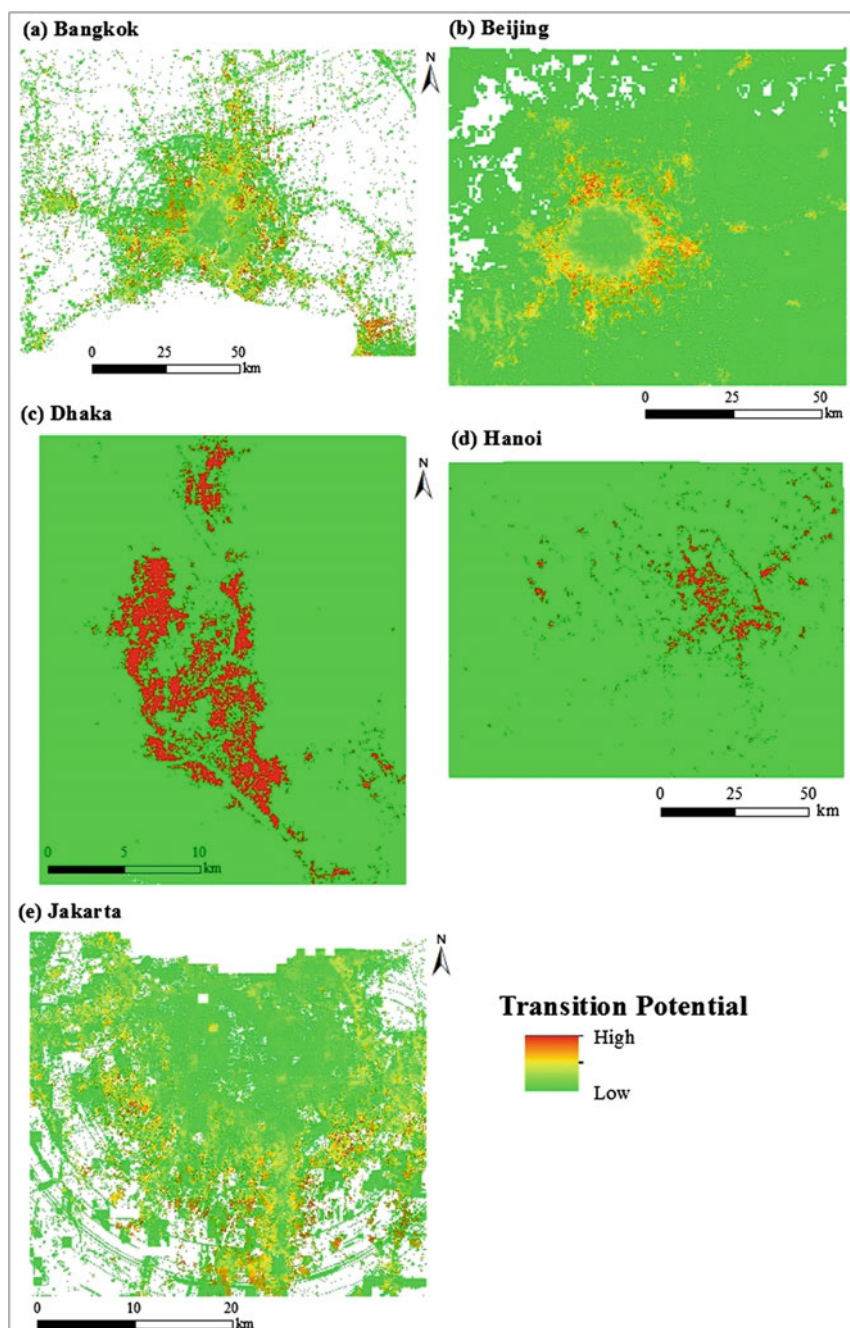


Fig. 2.1 Transition potential maps for Metropolitan Areas in Asia

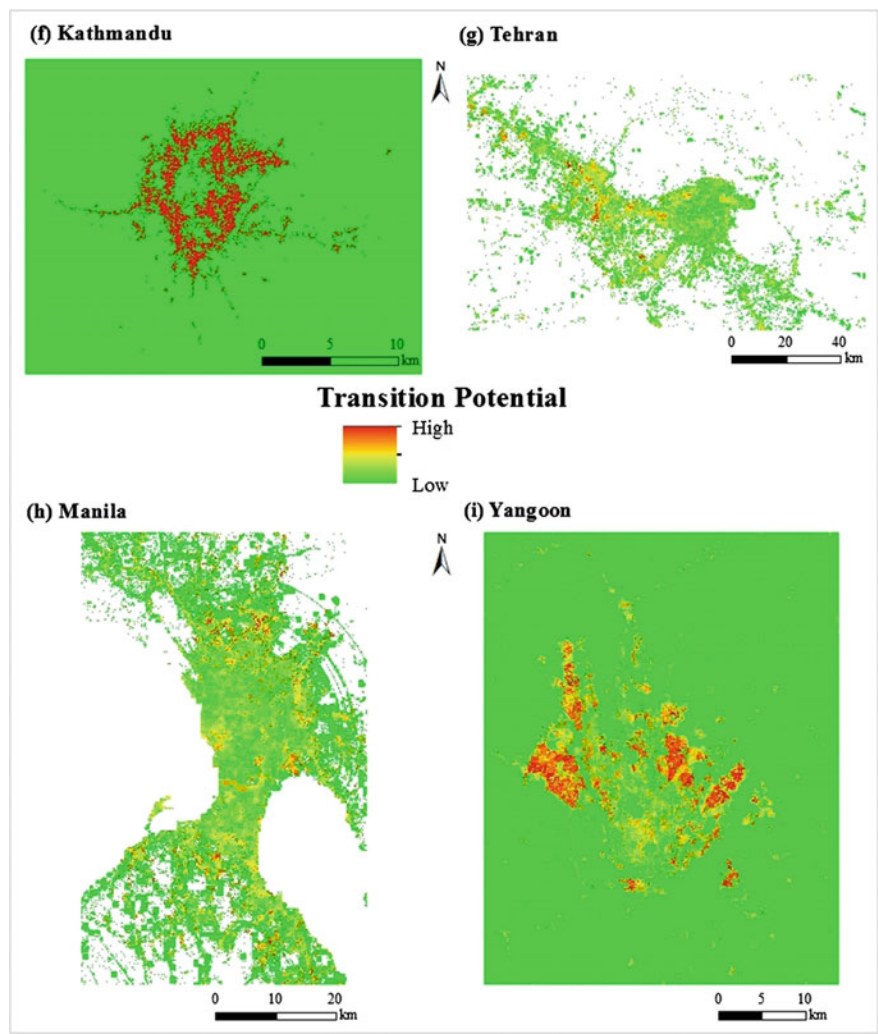


Fig. 2.1 (continued)

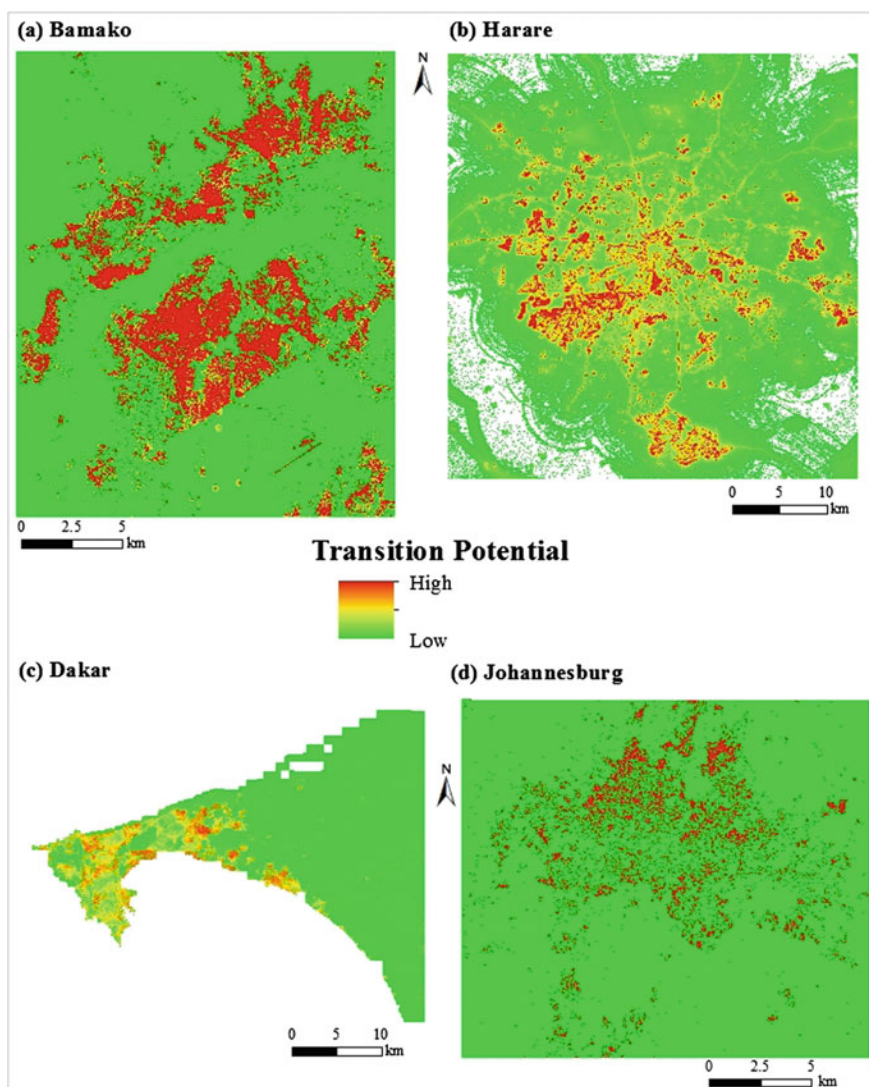


Fig. 2.2 Transition potential maps for Metropolitan Areas in Africa

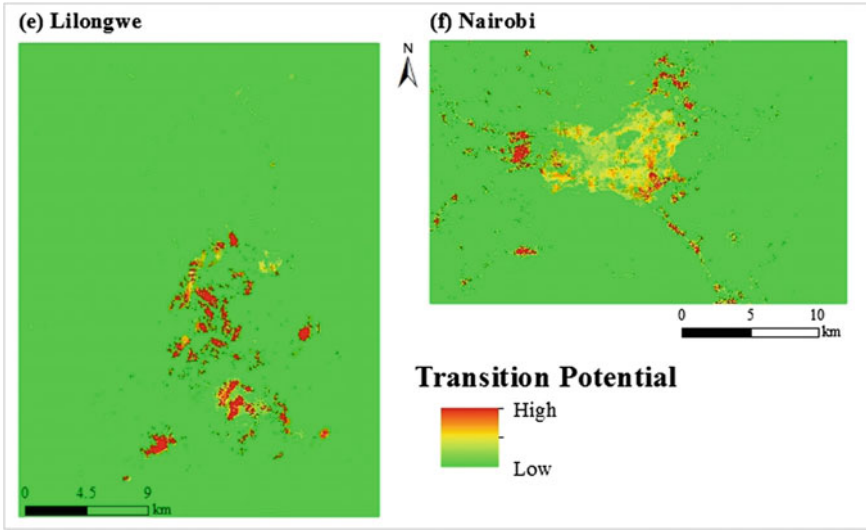


Fig. 2.2 (continued)

## 2.4 Results and Discussion

### 2.4.1 Evaluating the Goodness-of-Fit of Transition Potential Maps

#### 2.4.1.1 Metropolitan Areas in Asia

Figure 2.3 shows the TOC graphs for all transition potential models in Asia. The TOC statistic (Pontius and Si 2014) is an excellent method to assess the validity of a model, which predicts the location of the occurrence of a class by comparing a transition potential map depicting the likelihood of that class occurring (that is, the input map) and a reference image showing where that class actually exists (that is, the non-built-up to built-up change between 1990 and 2010). In particular, TOC offers a statistical analysis that shows how the class of interest is concentrated at the locations of relatively high transition potential for that class (Pontius and Si 2014). Therefore, TOC was used to evaluate the goodness-of-fit of calibration for transition potential maps derived from the BRT and RF models.

We focused our analysis on hits (that is, the correct “non-built-up to built-up” change), which were derived from the TOC statistic (Pontius and Si 2014). Generally, the Bangkok metropolitan area had 684.5 km<sup>2</sup> hits (representing 74% of the correctly predicted “non-built-up to built-up” changes) compared to 930.9 km<sup>2</sup> of the observed “non-built-up to built-up” changes between 1990 and 2010. For Beijing metropolitan area, the TOC statistics revealed that out of the 887.3 km<sup>2</sup> “non-built-up to built-up” changes that occurred between 1990 and 2010, only

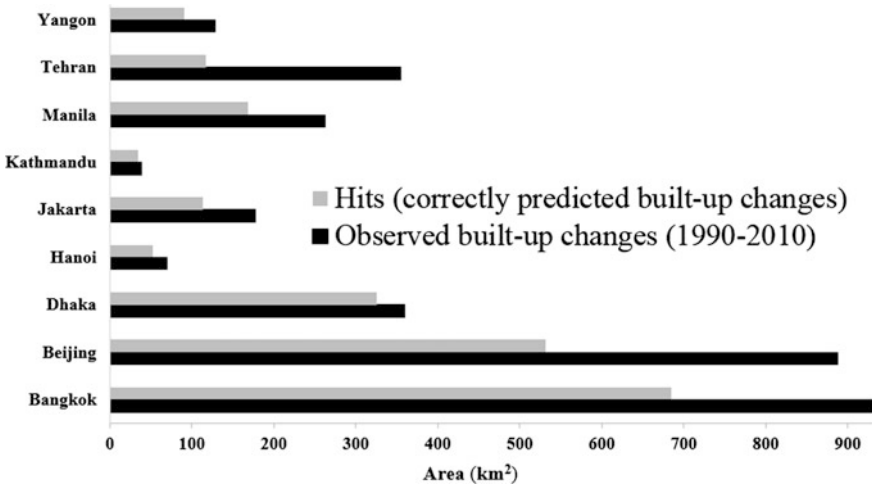


**Fig. 2.3** Hits versus observed changes for Asia based on TOC statistics

531.7 km<sup>2</sup> representing 60%, were correctly predicted. However, Dhaka metropolitan area had approximately 325.7 km<sup>2</sup> hits representing 91% compared to 359.4 km<sup>2</sup> of the observed “non-built-up to built-up” changes between 1990 and 2010. For Hanoi metropolitan area, the TOC statistics revealed that out of the 70.4 km<sup>2</sup> “non-built-up to built-up” changes that occurred between 1990 and 2010, 52.8 km<sup>2</sup> representing 75% were correctly predicted. The Jakarta metropolitan area had approximately 114 km<sup>2</sup> hits representing 64% compared to 177.2 km<sup>2</sup> of the observed “non-built-up to built-up” changes between 1990 and 2010 (validation period). For Kathmandu metropolitan area, the TOC statistics revealed that out of the 38.3 km<sup>2</sup> “non-built-up to built-up” changes that occurred between 1990 and 2010, only 34.1 km<sup>2</sup> representing 89% were correctly predicted. The Manila metropolitan area had approximately 169.2 km<sup>2</sup> (representing 65% of the correctly predicted “non-built-up to built-up” changes) compared to 262.2 km<sup>2</sup> of the observed “non-built-up to built-up” changes between 1990 and 2010. However, Tehran had the lowest hits. The TOC statistics revealed that out of the 354.7 km<sup>2</sup> observed “non-built-up to built-up” changes that occurred between 1990 and 2010, only 117.6 km<sup>2</sup> representing 33% were correctly predicted. The Yangon metropolitan area had approximately 91 km<sup>2</sup> hits representing 71% compared to 129 km<sup>2</sup> of the observed “non-built-up to built-up” changes between 1990 and 2010.

Generally, all models expect Tehran produced relatively good transition potential maps. However, all models were excellent at predicting the allocation of built-up and non-built-up persistence since built-up and non-built-up persistence accounts for approximately 70% of the metropolitan areas. This is reflected by the relatively high TOC values, which are all above 86% for all metropolitan areas.

### 2.4.1.2 Metropolitan Areas in Africa

Figure 2.4 shows the TOC graphs for all transition potential models in Africa. The Bamako metropolitan area had 50.7 km<sup>2</sup> hits (representing 78% of the correctly predicted “non-built-up to built-up” changes) compared to 65 km<sup>2</sup> of the observed “non-built-up to built-up” changes between 1990 and 2010. For Dakar metropolitan area, the TOC statistics revealed that out of the 66.8 km<sup>2</sup> “non-built-up to built-up” changes that occurred between 1990 and 2010, only 48.3 km<sup>2</sup> representing 72% were correctly predicted. The Harare metropolitan area had 170.8 km<sup>2</sup> hits representing 72% compared to 236.9 km<sup>2</sup> of the observed “non-built-up to built-up” changes between 1990 and 2010. Johannesburg metropolitan area had the highest number of hits. The TOC statistics revealed that out of the 648.2 km<sup>2</sup> “non-built-up to built-up” changes that occurred between 1990 and 2010, 578.8 km<sup>2</sup> representing 89% were correctly predicted. However, Lilongwe metropolitan area had the lowest number of hits. For example, 8.1 km<sup>2</sup> hits representing 36% compared to 22.7 km<sup>2</sup> of the observed “non-built-up to built-up” changes between 1990 and 2010 were observed. For Nairobi metropolitan area, the TOC statistics revealed that out of the 74.9 km<sup>2</sup> “non-built-up to built-up” changes that occurred between 1990 and 2010, only 43.3 km<sup>2</sup> representing 58% were correctly predicted.

Generally, five models (except Lilongwe) produced relatively good transition potential maps. However, all models were excellent at predicting the allocation of built-up and non-built-up persistence. This is reflected by the relatively high TOC values since built-up and non-built-up persistence is dominant in the metropolitan areas of Africa.

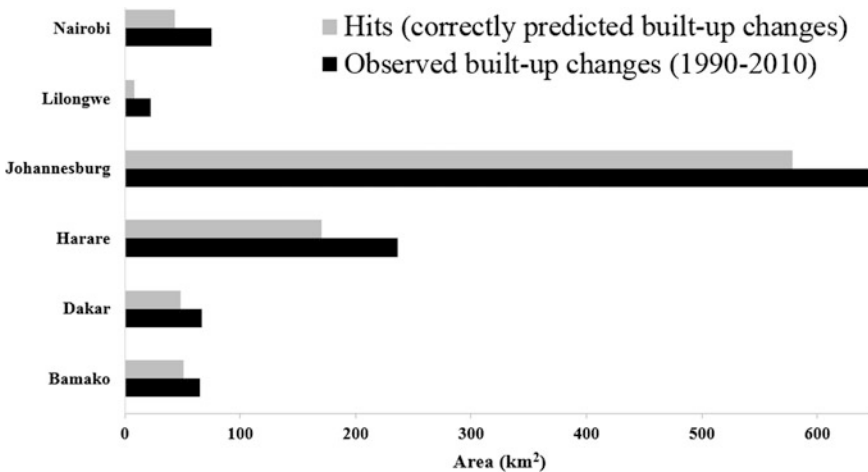


Fig. 2.4 Hits versus observed changes for Africa based on TOC statistics



2.4.2 Validation of the Simulated Land Use/Cover Changes

2.4.2.1 Metropolitan Areas in Asia

The observed and simulated land use/cover maps for all metropolitan areas in Asia are shown in Figs. 2.5, 2.6, 2.7, 2.8, 2.9, 2.10, 2.11, 2.12, and 2.13. Visual analysis shows that the BRT-CA and RF-CA models for Bangkok, Beijing, Dhaka, Hanoi, Jakarta, Kathmandu, Manila, and Yangon had good correspondence between the observed and simulated land use/cover maps for 2014 (Figs. 2.5, 2.6, 2.7, 2.8, 2.9, 2.10, 2.11, 2.12, and 2.13). The spatial patterns of built-up areas simulated by the BRT-CA and RF-CA models resemble the observed built-up patterns to a large

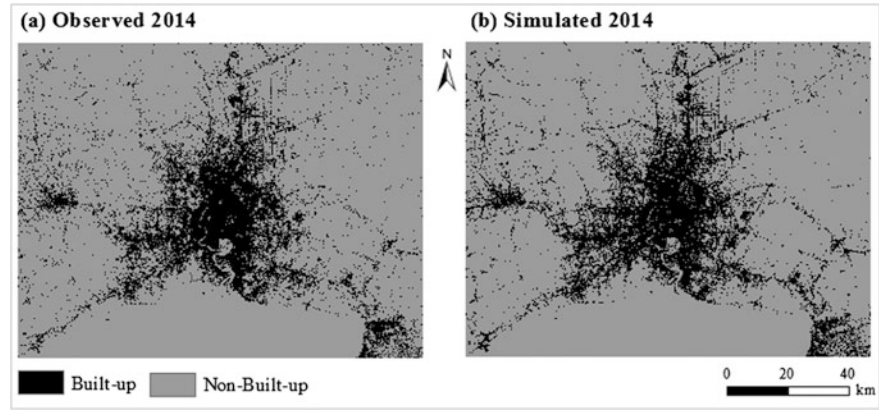


Fig. 2.5 Comparison of observed versus simulated land use/cover for Bangkok

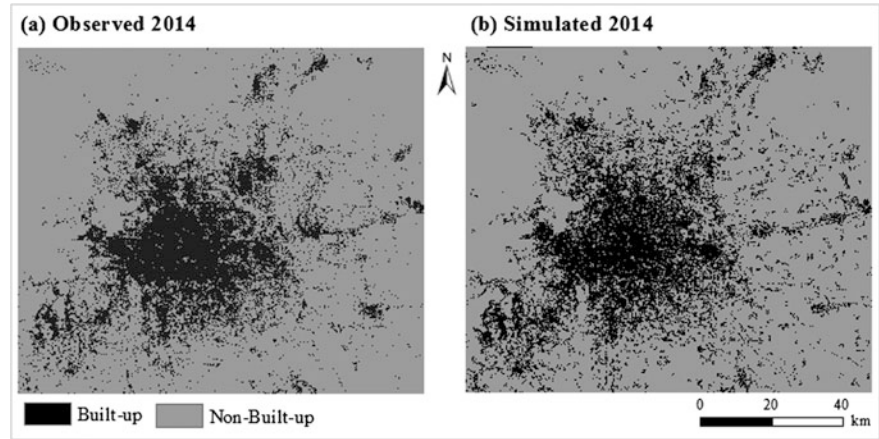


Fig. 2.6 Comparison of observed versus simulated land use/cover for Beijing



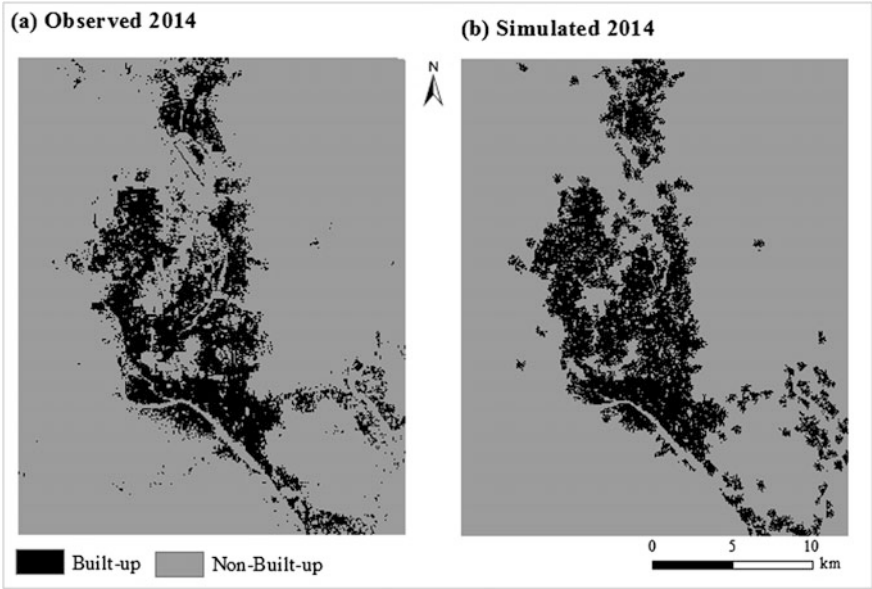


Fig. 2.7 Comparison of observed versus simulated land use/cover for Dhaka

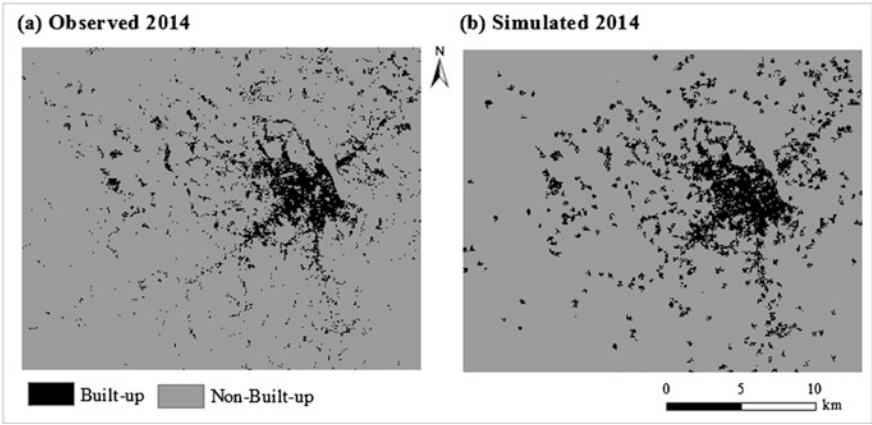
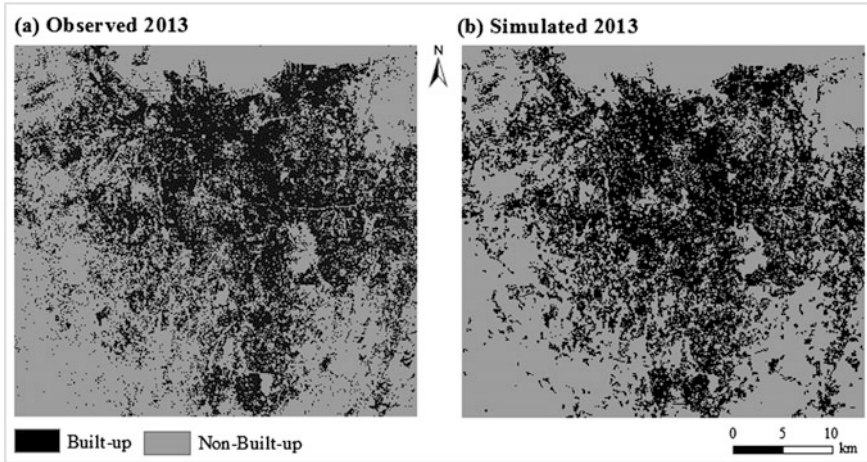


Fig. 2.8 Comparison of observed versus simulated land use/cover for Hanoi

extent. This suggests that the BRT-CA and RF-CA models were relatively accurate at allocating “non-built-up to built-up” changes.

However, Fig. 2.12 shows relatively medium correspondence between the simulated built-up patterns and the observed built-up patterns for Tehran. Generally, there was an underprediction of the built-up class for Tehran metropolitan area. This is partly attributed to lower spatial allocation of



**Fig. 2.9** Comparison of observed versus simulated land use/cover for Jakarta

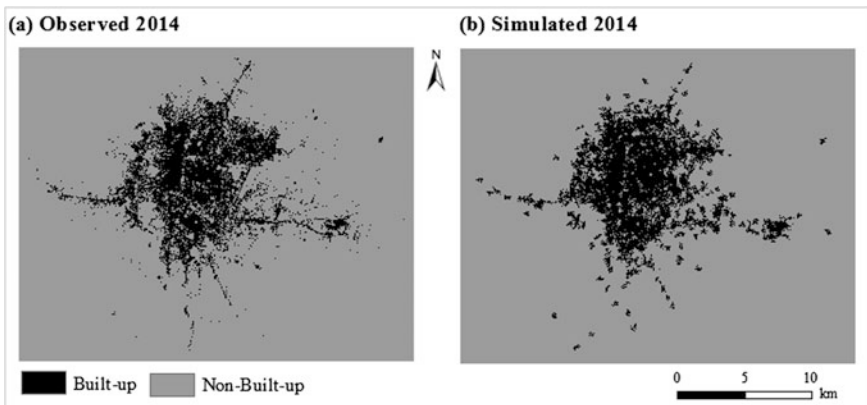


**Fig. 2.10** Comparison of observed versus simulated land use/cover for Kathmandu

“non-built-up to built-up” changes that was observed during the calibration of the RF model for Tehran metropolitan area (Fig. 2.1g). In addition, it should be noted that Tehran metropolitan area has quite a unique setting with very high landscape fragmentation and scattered urban development, which makes it challenging to develop a robust simulation model. Nonetheless, it is also important to note that some of the allocated built-up areas had strong agreement between the simulated and observed land use/cover maps, which means that the CA model can be used to simulate future land use/cover changes.

For quantitative model validation, we used the observed (initial) land use/cover map for 1990, the observed (reference) land use/cover map for 2014, and the simulated land use/cover map for 2014. Table 2.5 shows the validation statistics

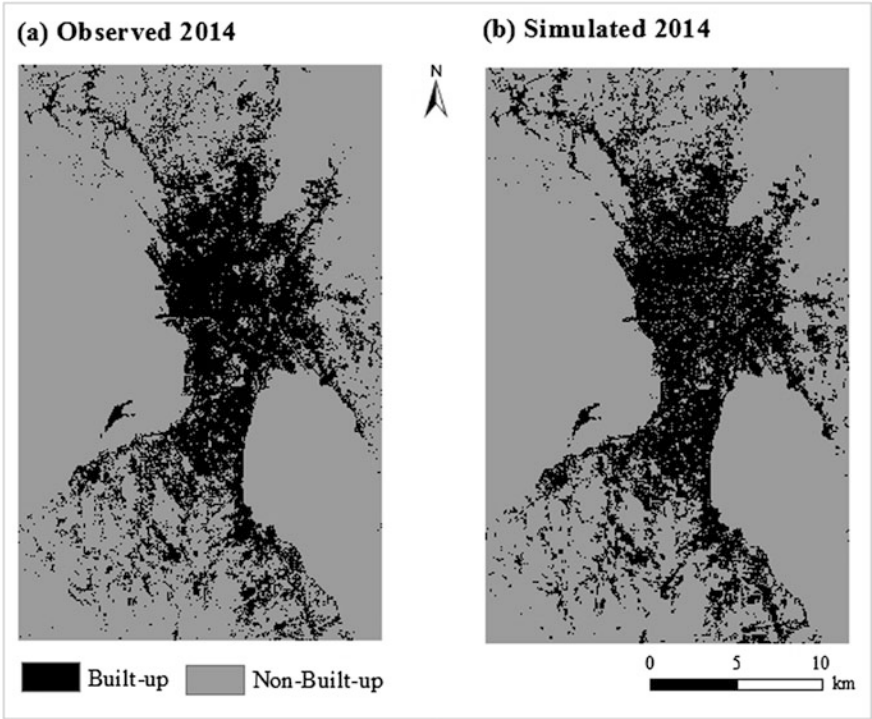


**Fig. 2.11** Comparison of observed versus simulated land use/cover for Manila

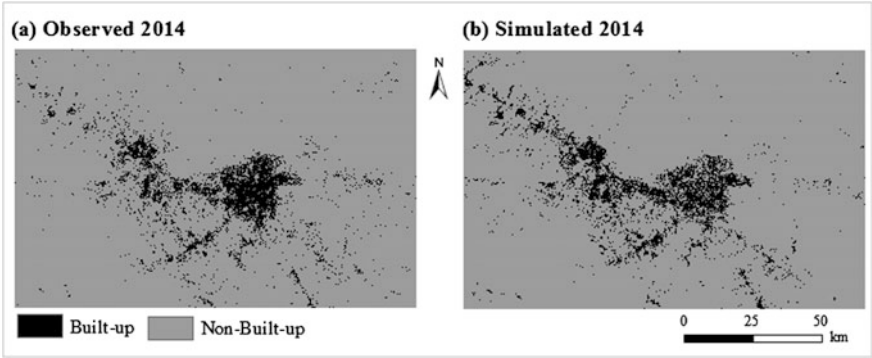


**Fig. 2.12** Comparison of observed versus simulated land use/cover for Tehran

based on KSimulation, KTranslocation, KTransition, and the FoM for all metropolitan areas in Asia. KSimulation values range from 42 to 69%, while the KTranslocation values range from 44 to 71% (Table 2.5). Tehran had the lowest KSimulation and KTranslocation scores, while Dhaka had the highest KSimulation and KTranslocation scores. The FoM statistics also follow the similar pattern as the

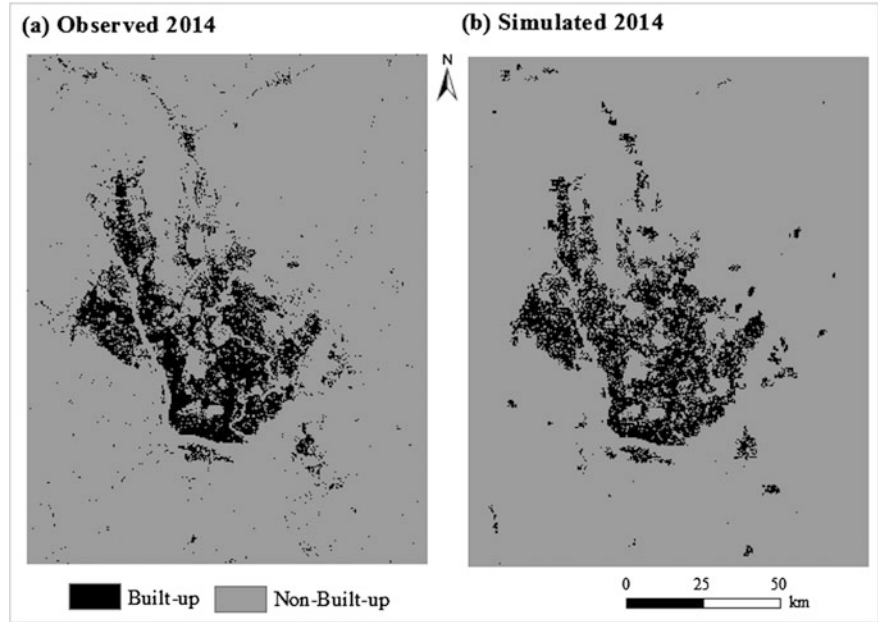


**Fig. 2.13** Comparison of observed versus simulated land use/cover for Yangon

**Table 2.5** Validation statistics for all simulation models in Asia

Metropolitan area	KSimulation	KTranslocation	KTransition	Figure of merit (%)
Bangkok	0.62	0.61	0.95	51
Beijing	0.51	0.55	0.93	45
Dhaka	0.69	0.71	0.97	58
Hanoi	0.56	0.67	0.83	42
Jakarta	0.47	0.49	0.96	43
Kathmandu	0.68	0.68	0.98	55
Manila	0.60	0.64	0.94	48
Tehran	0.42	0.44	0.96	29
Yangon	0.62	0.63	0.98	48

KSimulation and KTranslocation statistics. These results are in agreement with the goodness-of-fit transition potential results (Fig. 2.2), which suggest that transition potential maps have more influence in the overall accuracy of the CA simulation models. A study by Pontius et al. (2007, 2008) revealed that the FoM observed in other LCMs ranged from 1 to 59%. Therefore, the accuracy of the BRT-CA and RF-CA models are relatively high since the FoM is within the upper range of previously observed LCMs (Kamusoko and Gamba 2015).

Generally, all the simulation models had high KTransition score, which are above 83%. This is supported by the quantitative analysis between the simulated and observed land use/cover changes for all metropolitan areas in Asia. For example, a quantitative comparison for Bangkok revealed that the observed and projected quantities of built-up were 2292.4 and 2428.5 km<sup>2</sup>, respectively. For Beijing, the observed built-up class was 2173.7 km<sup>2</sup>, whereas the corresponding simulated class was 2364.1 km<sup>2</sup>. However, the observed built-up class was 118.5 km<sup>2</sup>, while the corresponding simulated class was 171.8 km<sup>2</sup> for Dhaka. For Hanoi, the observed built-up class was 133.3 km<sup>2</sup>, whereas the corresponding simulated class was 171.8 km<sup>2</sup>. In the case of Jakarta, the observed built-up class was 623.5 km<sup>2</sup>, while the corresponding simulated class was 606.8 km<sup>2</sup>. For Kathmandu, the observed built-up class was 75.9 km<sup>2</sup>, whereas the corresponding simulated class was 76 km<sup>2</sup>. Nevertheless, the observed built-up class was 848.6 km<sup>2</sup>, while the corresponding simulated class was 984.6 km<sup>2</sup> for Manila. For Tehran, the observed built-up class was 923.3 km<sup>2</sup>, whereas the corresponding simulated class was 969.1 km<sup>2</sup>. Last but not least, the observed built-up class was 228.9 km<sup>2</sup>, while the corresponding simulated class was 223.1 km<sup>2</sup> for Yangon. These results show that all simulation models were relatively accurate for simulating land use/cover quantity.

#### 2.4.2.2 Metropolitan Areas in Africa

The observed and simulated land use/cover maps for all metropolitan areas in Africa are shown in Figs. 2.14, 2.15, 2.16, 2.17, 2.18, and 2.19. Visual analysis

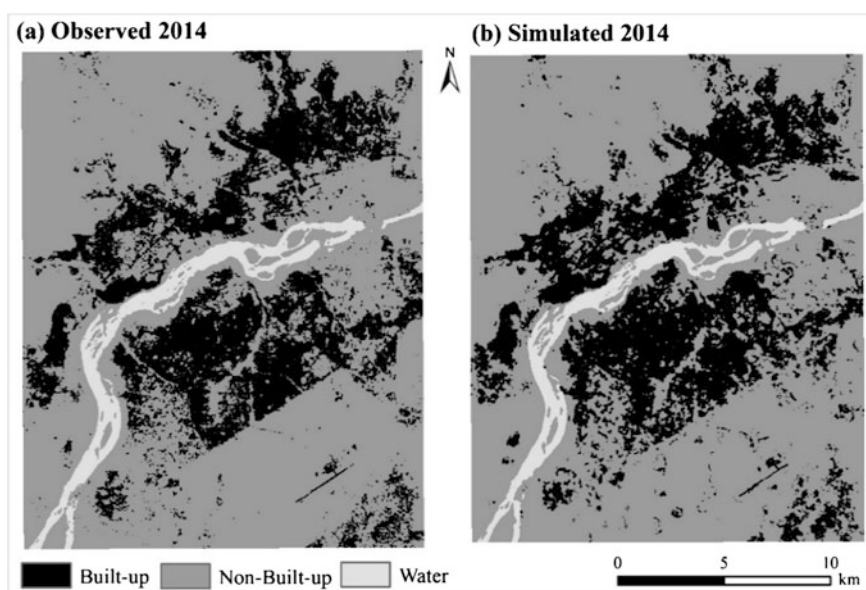


**Fig. 2.14** Comparison of observed versus simulated land use/cover for Bamako



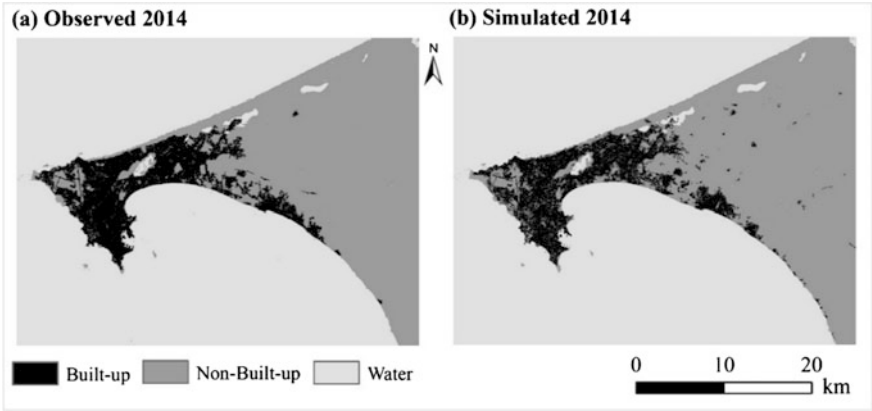


**Fig. 2.15** Comparison of observed versus simulated land use/cover for Dakar

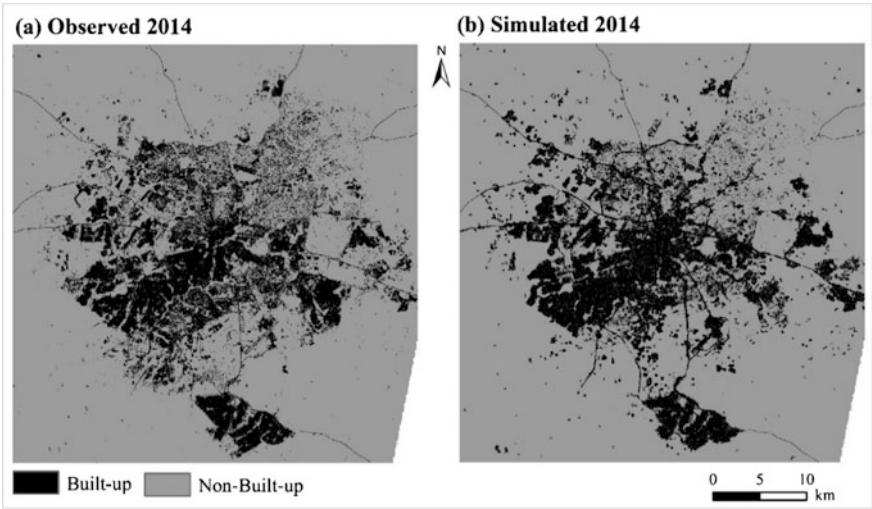


**Fig. 2.16** Comparison of observed versus simulated land use/cover for Harare

shows that the BRT-CA and RF-CA models for all metropolitan areas had a relatively high correspondence between the observed and simulated land use/cover maps for 2014 (Figs. 2.14, 2.15, 2.16, 2.17, 2.18, and 2.19). Generally, the spatial patterns of the simulated built-up areas closely match the observed built-up patterns. While a slight degree of clumpiness is noted in some metropolitan areas such as Harare, in general the BRT-CA and RF-CA models were relatively good at allocating “non-built-up to built-up” changes and simulating land use/cover (Figs. 2.14, 2.15, 2.16, 2.17, 2.18, and 2.19). This attributed to the rigorous calibration of the transition potential maps, which were computed using BRT and RF

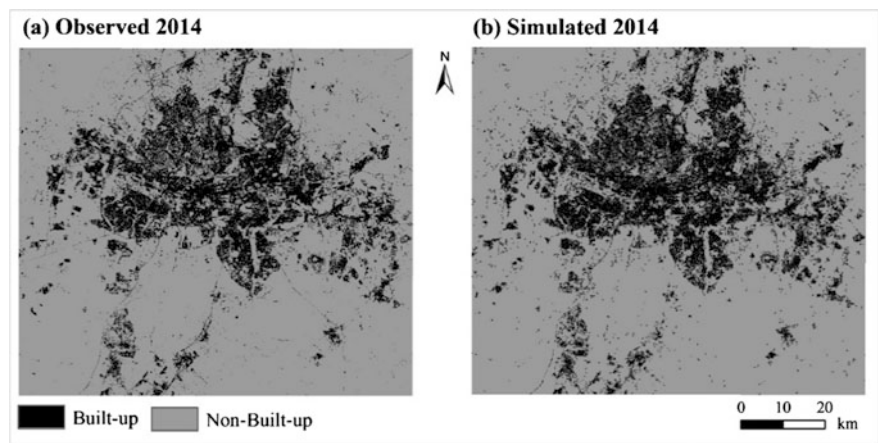


**Fig. 2.17** Comparison of observed versus simulated land use/cover for Johannesburg

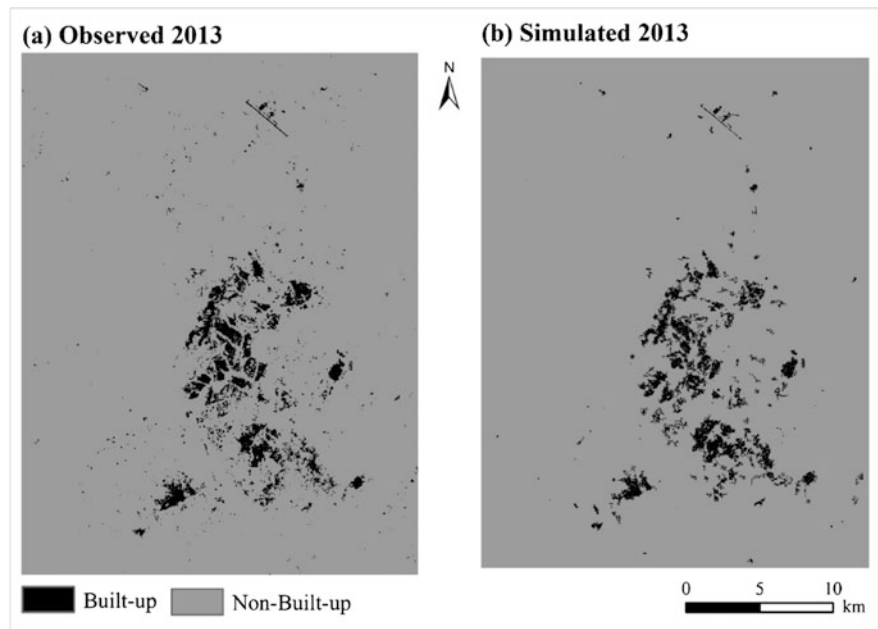


**Fig. 2.18** Comparison of observed versus simulated land use/cover for Lilongwe

models (Fig. 2.3). These simulation results are significant given that all the BRT and RF models only incorporated a limited number of driving factors. Therefore, BRT-CA and RF-CA models can be used to simulate future land use/cover changes.

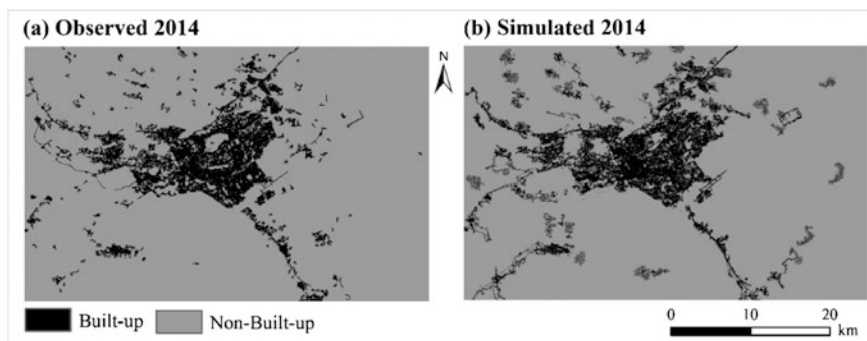


**Fig. 2.19** Comparison of observed versus simulated land use/cover for Nairobi

**Table 2.6** Validation statistics for all simulation models in Africa

Metropolitan area	KSimulation	KTranslocation	KTransition	Figure of merit (%)
Bamako	0.72	0.75	0.96	63
Dakar	0.75	0.79	0.94	62
Harare	0.49	0.50	0.99	47
Johannesburg	0.66	0.70	0.96	55
Lilongwe	0.68	0.70	0.97	53
Nairobi	0.56	0.60	0.93	43

Table 2.6 shows the validation statistics based on KSimulation, KTranslocation, KTransition, and the FoM. Bamako, Dakar, Johannesburg, Lilongwe, and Nairobi had KSimulation and KTranslocation scores above 50% (Table 2.6). All the simulation models had high KTransition score (above 93%), which is higher than the simulation models in metropolitan areas of Asia. This is supported by the quantitative analysis between the simulated and observed land use/cover changes for all metropolitan areas in Africa. For example, a quantitative comparison for Bamako revealed that the observed and simulated built-up class was 104.7 and 111.9 km<sup>2</sup>, respectively. While the observed built-up class was 118.6 km<sup>2</sup>, the corresponding simulated class was 109.7 km<sup>2</sup> for Dakar. However, the observed built-up class was 358.6 km<sup>2</sup>, while the corresponding simulated class was 360.4 km<sup>2</sup> for Harare. For Johannesburg, the observed built-up class was 1418.6 km<sup>2</sup>, whereas the corresponding simulated class was 1494.6 km<sup>2</sup>. Although Lilongwe had a relatively lower accuracy for the transition potential (Table 2.6), the observed built-up class was 34.7 km<sup>2</sup>, while the corresponding simulated class was 32.9 km<sup>2</sup>. For Nairobi, the observed built-up class was 182.8 km<sup>2</sup>, whereas the corresponding simulated class was 198.9 km<sup>2</sup>. These results indicate that all simulation models were relatively accurate for simulating land use/cover quantity. This is supported by the high FoM, which was above 43% for all simulation models in Africa.



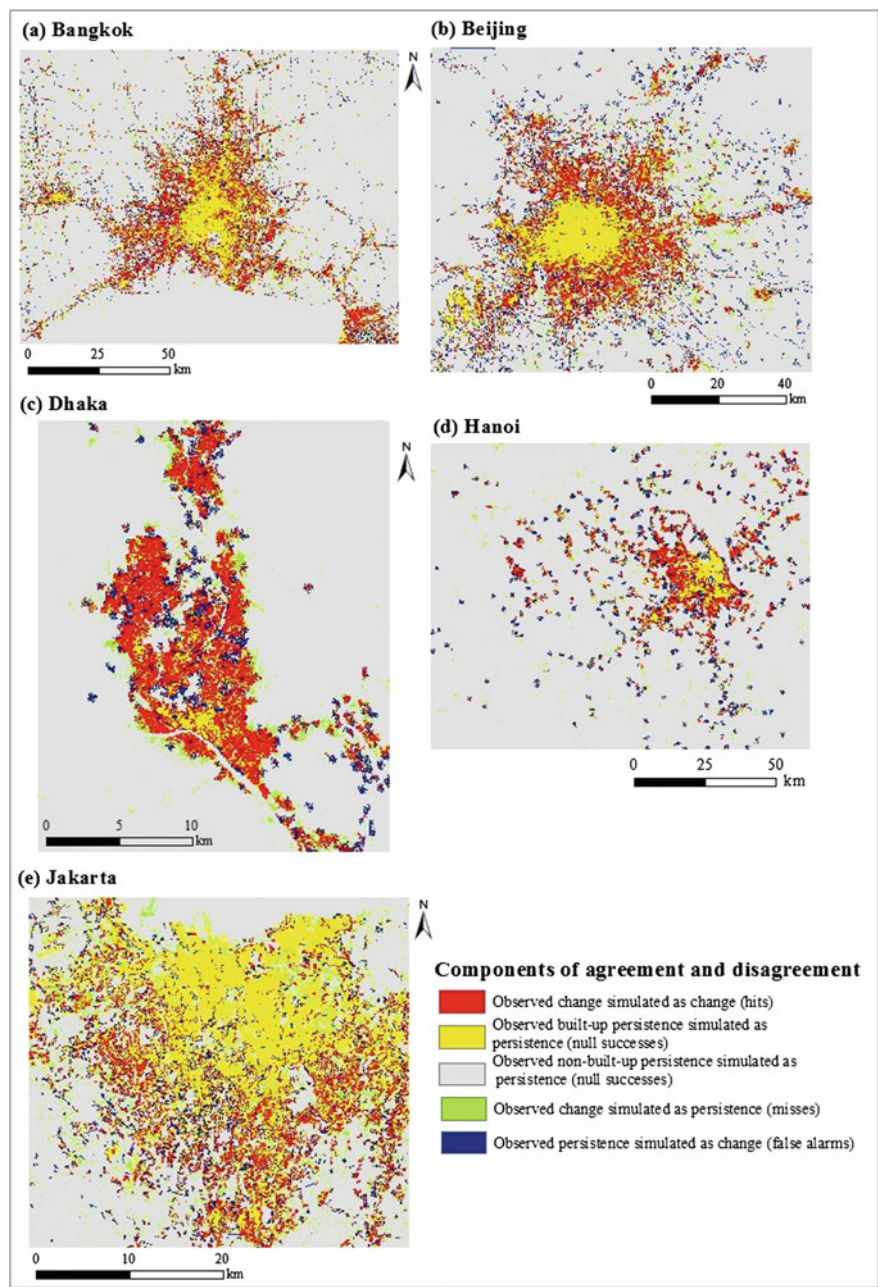


Fig. 2.20 Components of agreement and disagreement for Asia

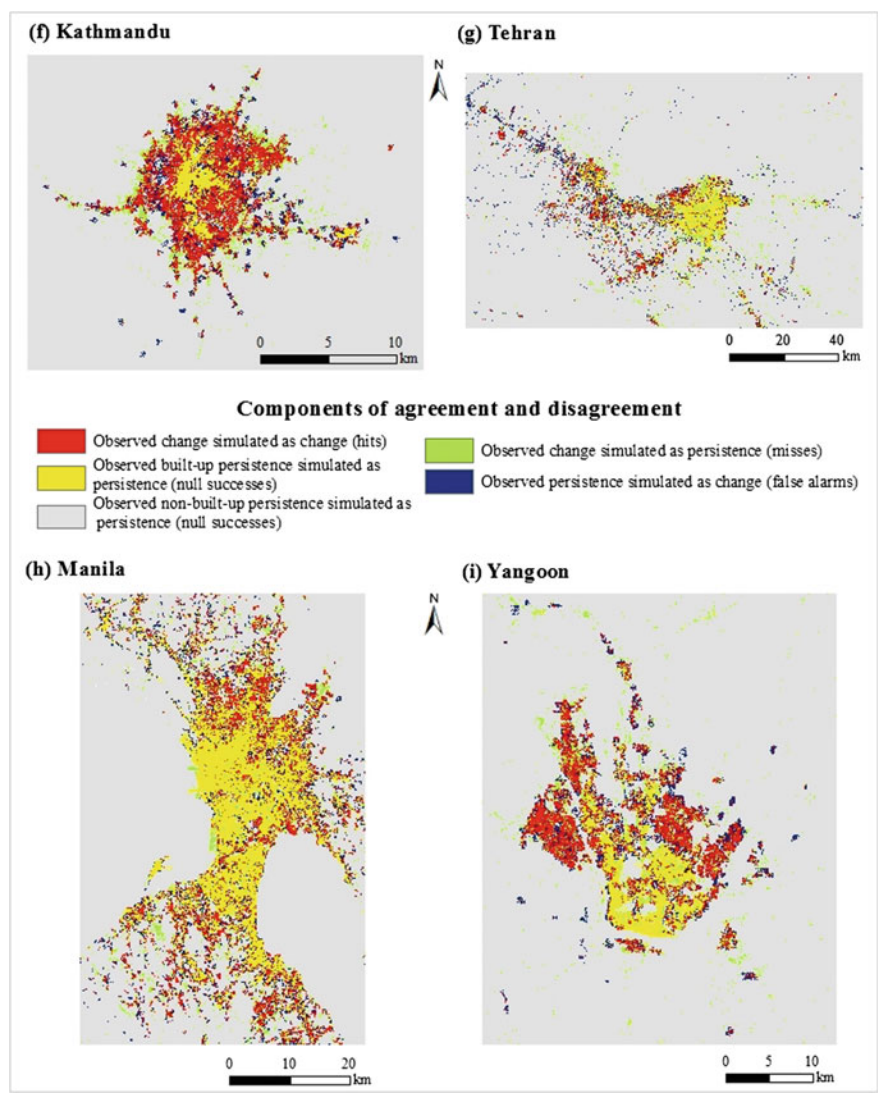
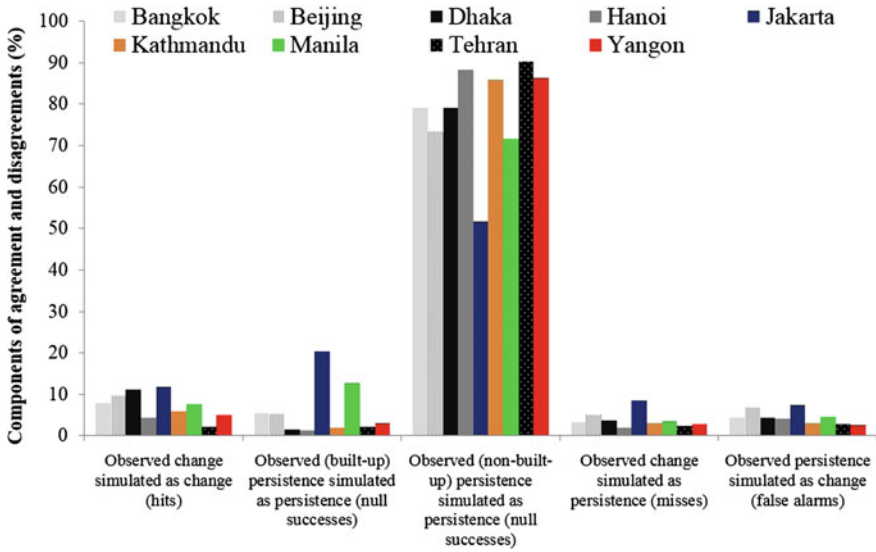


Fig. 2.20 (continued)

2.4.3 Analysis of Components of Agreement and Disagreement

2.4.3.1 Metropolitan Areas in Asia

Figures 2.20 and 2.21 show the components of agreement and disagreement based on the overlay of the initial (1990), the observed (2014), and simulated land



**Fig. 2.21** Components of agreement and disagreement expressed as a percentage (Asia)

use/cover maps (2014) for all models. The components of agreement and disagreement reveal information such as: (1) observed change simulated correctly as change (hits); (2) observed persistence (built-up and non-built-up) simulated correctly as persistence (null successes); (3) observed change simulated wrongly as persistence (misses); and (4) observed persistence simulated wrongly as change (false alarms).

Results show that non-built-up persistence had the largest components of agreement for all the models in Asia (Figs. 2.20 and 2.21). This is because non-built-up persistence occupied about 60% of the metropolitan areas between 1990 and 2010. However, there are variation in terms of the hits, false alarms, and misses. For example, Bangkok, Dhaka, Kathmandu, Manila, and Yangon had the same or slightly more hits than the combined misses and false alarms (Figs. 2.20 and 2.21). This is encouraging since it shows that BRT-CA and RF-CA models performed relatively well. While Beijing, Hanoi, Jakarta, and Tehran had slightly more combined misses and false alarms than hits, the BRT-CA and RF-CA models also performed relatively well.

While the results show improvement in the LCMs, it must be noted that the simulated land use/cover maps include uncertainty of the original land use/cover maps, especially the 1990 land use/cover map (which was not quantitatively validated). In addition, it was observed that the BRT-CA and RF-CA models failed to simulate unconnected newly built-up areas, which is clearly apparent in the components of agreement and disagreement (Fig. 2.21). This is attributed to spatial and temporal nonstationarity in the built-up change process. Figure 2.22 shows the normalized observed built-up change rate between different epochs in Asia, which

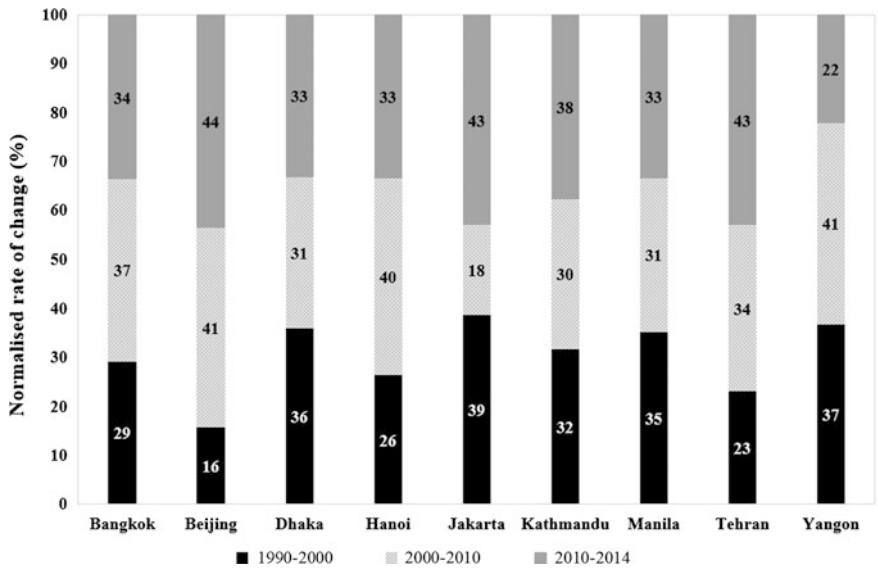


**Fig. 2.22** Normalized observed built-up change rate between different epochs in Asia

indicates clearly that built-up changes for all metropolitan areas were nonstationary. The combination of rapid and slow urban growth developments between different time periods (e.g., “1990–2000” and “2000–2010” periods) is challenging for simulating unconnected newly built-up areas based on BRT-CA and RF-CA models. This is because statistical or machine learning algorithms have difficulty in handling nonstationarity (The Sate of Land Change Modeling 2014).

**2.4.3.2 Metropolitan Areas in Africa**

For Africa, non-built-up persistence had the largest components of agreement for all the models as was observed in Asia (Figs. 2.23 and 2.24). This is because non-built-up persistence occupied more than 50% of the metropolitan areas between 1990 and 2010. Furthermore, Bamako, Dakar, Johannesburg, Lilongwe, and Nairobi metropolitan areas had slightly more hits than the combined misses and false alarms (Figs. 2.23 and 2.24), indicating that the RF-CA model performed relatively well. However, Harare metropolitan area had more combined misses and false alarms than hits. This is because the RF model failed to predict unconnected newly built-up areas, particularly in unplanned and illegal settlement areas. In addition, uncertainty is increased due to the high-temporal nonstationarity (Fig. 2.25). Consequently, the RF model had difficulty modeling the unbalanced land outcomes, namely the combination of rapid and slow urban growth

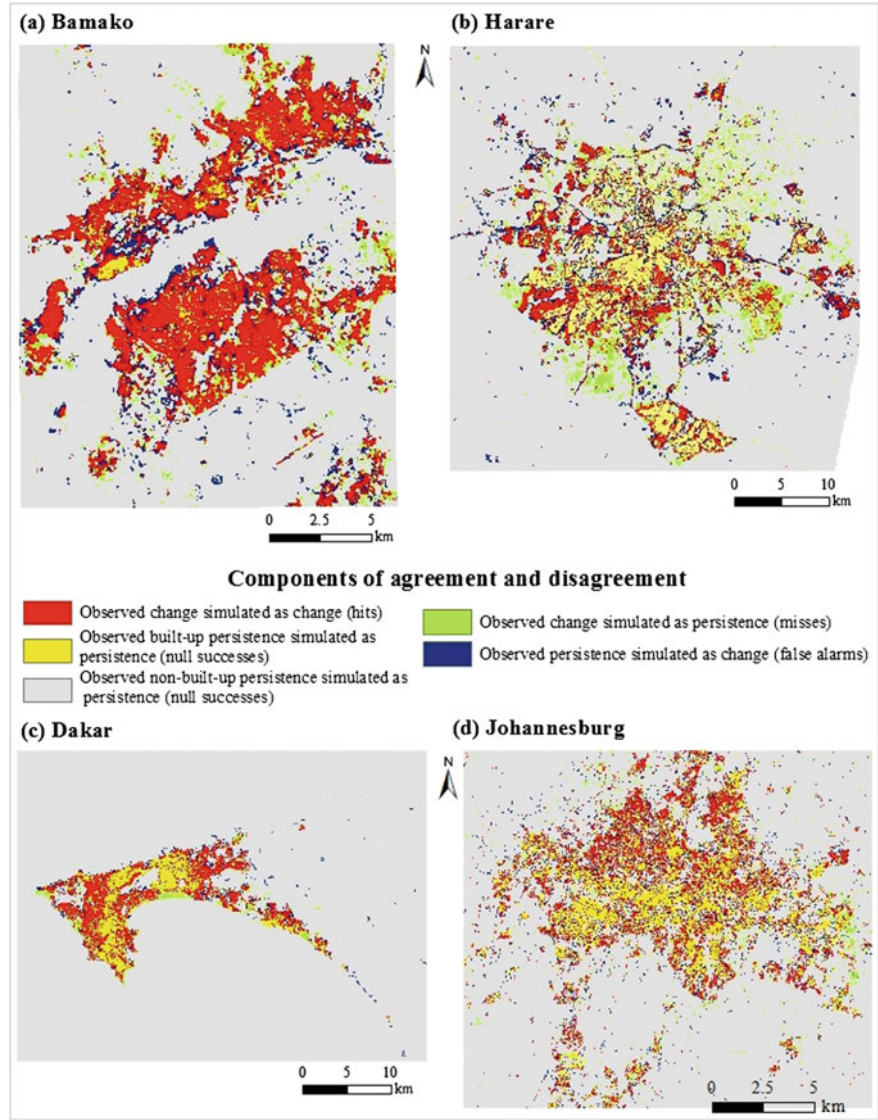


Fig. 2.23 Components of agreement and disagreement for Africa

developments, which occurred during the “1990–2000” and “2000–2010” periods (Fig. 2.25). For example, the rate of “non-built-up to built-up” change between 1990 and 2000 was approximately 114.4 km<sup>2</sup>, while the “non-built-up to built-up” change slowed to 69.8 km<sup>2</sup> between 2000 and 2010 (Kamusoko and Gamba 2015).



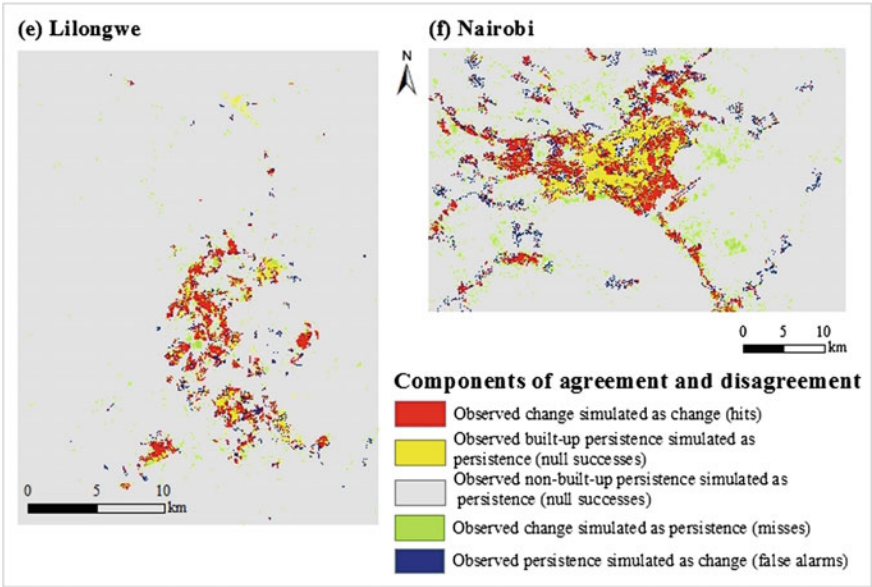


Fig. 2.23 (continued)

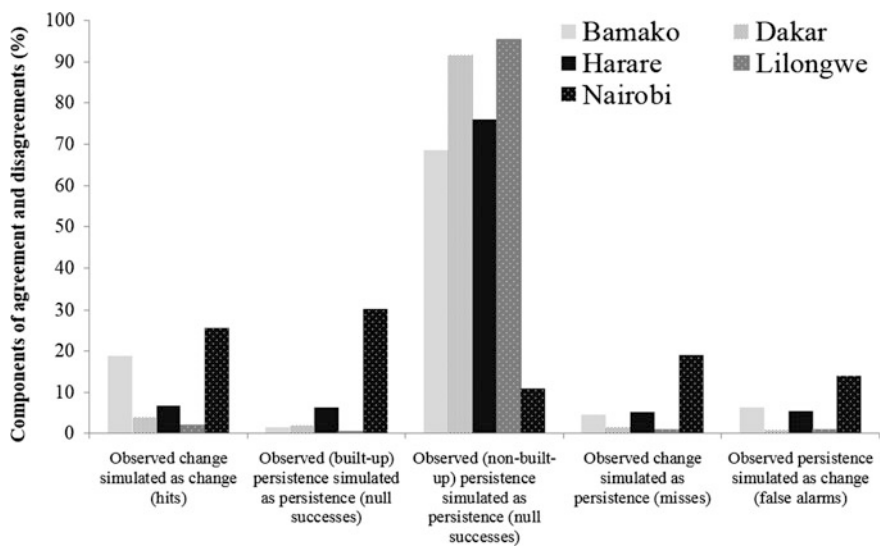


Fig. 2.24 Components of agreement and disagreement expressed as a percentage (Asia)

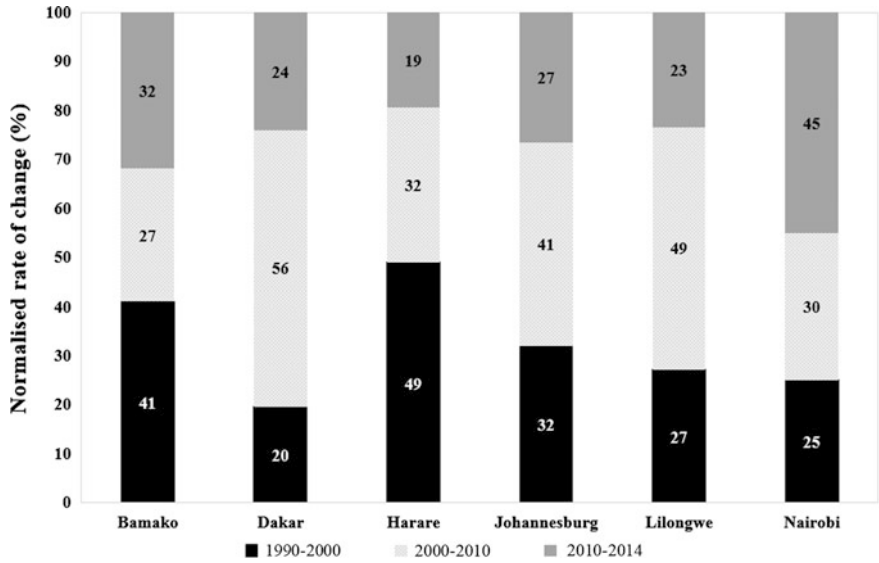


Fig. 2.25 Normalized observed built-up change rate between different epochs in Africa

### 2.5 Capturing Spatial Pattern of Urbanization

In order to capture, examine, and compare the spatial pattern of urbanization in all the cities, we used five spatial metrics. These include PLAND, PD, ENN, CIRCLE, and SHAPE (Table 2.7). This set of spatial metrics was also used recently by the Asian Development Bank (ADB) in a study entitled “Urban Metabolism of Six Asian Cities” (ADB 2014).

In this analysis, all these five spatial metrics were used at the class level (built-up). The 8-cell neighbor rule was used to determine the membership of each pixel to a patch. In this rule, all the four orthogonal and four diagonal neighbors of the focal cell are used. In the 8-cell neighbor rule, two cells of the same LULC class that are diagonally touching are considered as part of the same patch, but in the case of the 4-cell neighbor rule, these are considered separate patches (McGarigal et al. 2012). We selected the 8-cell neighbor as it has been used in various studies (e.g., Townsend et al. 2009; Estoque and Murayama 2013, 2016; Estoque et al. 2014). The five spatial metrics were computed using FRAGSTATS 4.2 (McGarigal et al. 2012).

**Table 2.7** List and details of the class-level (built-up) spatial metrics used

Spatial metrics	Range	Unit	Description	Measure
PLAND	$0 < \text{PLAND} \leq 100$	Percent	Percentage of landscape; percentage of built-up relative to the whole landscape (excluding water)	Area
PD	$\text{PD} > 0$	Number per 100 ha or per $\text{km}^2$	Patch density; number of patches of built-up per unit area	Aggregation (subdivision/fragmentation)
ENN (mean)	$\text{ENN} > 0$	Meter	Euclidean nearest neighbor distance; distance to the nearest neighboring patch of the same type, based on shortest edge-to-edge distance	Aggregation (isolation/dispersion)
CIRCLE (mean)	$0 \leq \text{CIRCLE} < 1$	None	Related circumscribing circle; provides a measure of overall patch elongation; measures the circularity of built-up patches. Low values represent circular patches	Shape (geometry)
SHAPE (mean)	$1 \leq \text{SHAPE} \leq \infty$	None	Shape index; measures the complexity of patch shape compared to a standard shape (square) of the same size; measures the irregularity of built-up patches. Low values represent low complexity	Shape (complexity)

Source McGarigal et al. (2012). Note The water class was not included in the derivation of the metrics



## 2.6 Summary and Conclusions

Taking the selected metropolitan areas in Asia and Africa, the purpose of this chapter was to describe the methodology used to produce the land use/cover maps, calibrate and validate LCMs. The specific objectives of this chapter were to evaluate the goodness-of-fit of transition potential maps, validate the simulated land use/cover maps as well as elucidate components of agreement and disagreement. Land use/cover maps were classified from Landsat imagery for 1990, 2000, 2010, and 2014 using the (RF) classifier. Finally, land use/cover changes were simulated based on the BRT-CA and RF-CA models.

Quantitative accuracy assessment for the 1990 land use/cover maps was not conducted because of the unavailability of reference data such as aerial photographs and high-resolution satellite imagery. However, the Atlas of Urban Expansion developed by the Lincoln Institute of Land Policy (Angel et al. 2010) was used to visually check the quality of land use/cover maps for the 1990 epoch (that is, Landsat imagery acquired between 1988 and 1993). Qualitative and quantitative accuracy assessments were conducted for land use/cover maps from 2000, 2010, and 2014 epochs based on very high-resolution images (e.g., QuickBird image) from Google Earth™. Overall land use/cover classification accuracy for all land use/cover maps ranged from 70 to 90% for all the metropolitan areas.

Generally, the BRT-CA and RF-CA models for all metropolitan areas in Asia and Africa performed relatively well. However, the BRT-CA and RF-CA models for metropolitan areas in Africa performed better than the BRT-CA and RF-CA models for metropolitan areas in Asia. The modeling and simulation results presented in this chapter—however limited to selected case studies in Asia and Africa—provide an initial exploration of the machine learning-cellular (ML-CA) models for land change modeling. While urban expansion in Asia and Africa has been acknowledged, to-date spatial LCMs have not been rigorously explored and validated. Of particular importance here is the possibility of improving transition potential modeling using machine learning models. Consequently, this chapter highlights the value and significance of robust calibration, validation and simulation of spatial LCMs—in particular ML-CA models—for the 15 metropolitan areas in Asia and Africa. Therefore, this chapter provides a foundation for calibrating and validating spatial LCMs.

While the simulation results are encouraging, it is also important to acknowledge that all the BRT-CA and RF-CA models fail to simulate newly developed or built-up areas, which are not connected to existing urban built-up areas. Previous studies revealed that statistical or machine learning models underpredict the location of new patches, which are not connected to existing built-up areas (Pontius and Malanson 2005) due to spatial or temporal nonstationarity (Estoque and Murayama 2014; The State of Land Change Modeling 2014). Therefore, issues related to nonstationarity need to be addressed using more temporal land use/cover data (e.g., at 5 year intervals) or combining BRT-CA and RF-CA models with other LCMs. Although some model uncertainties remain, the BRT-CA and RF-CA models

developed in this study have potential to improve land change modeling in general, and urban growth modeling and simulation in particular. Given the broader implications of the results from this chapter, further studies should be carried out to test the BRT-CA and RF-CA models using multiple temporal land use/cover maps at a shorter time interval in order to minimize the effects on spatial and temporal nonstationarity.

## References

- ADB (Asian Development Bank) (2014) Republic of the Philippines national urban assessment. Asian Development Bank, Metro Manila, Philippines
- Angel SJ, Parent DL, Civco Blei AM (2010) Atlas of urban expansion. Lincoln Institute of Land Policy, Cambridge, MA
- Batty M (1998) Urban evolution on the desktop: simulation with the use of extended cellular automata. *Environ Plan B* 30:1943–1967
- Batty M, Xie Y (2005) Urban growth using cellular automata models. In: Maguire DJ, Batty M, Goodchild MF (eds) GIS, spatial analysis, and modelling. ESRI Press, CA, USA, pp 151–172
- Bhaduri B, Bright E, Coleman P, Urban M (2007) LandScan USA: a high resolution geospatial and temporal modeling approach for population distribution and dynamics. *Geo J* 69:103–117
- Breiman L (2001) Random forests. *Mach Learn* 45:5–32
- Cheng J, Masser I (2004) Understanding spatial and temporal processes of urban growth: cellular automata modelling. *Environ Plan B* 31:167–194
- Clarke KC, Hoppen S, Gaydos L (1997) A Self-modifying cellular automaton model of historical urbanization in the San Francisco Bay Area. *Environ Plan B* 24:247–261
- Couclelis H (1985) Cellular worlds: a framework for modeling micro-macro dynamics
- Couclelis H (1989) Macrostructure and microbehavior in a metropolitan area. *Environ Plann* 16:141–154
- Dale VH (1997) The relationship between land-use change and climate change. *Ecol Appl* 17:753–769
- Eastman JR, Solorzano LA, Van Fossen ME (2005) Transition potential modeling for land-cover change. In: Maguire DJ, Batty M, Goodchild MF (eds) GIS, spatial analysis, and modelling. ESRI Press, CA, USA, pp 357–385
- Elith J, Leathwick JR, Hastie T (2008) A working guide to boosted regression trees. *J Anim Ecol* 77:802–813
- Engelen G (1988) The theory of self-organization and modeling complex urban systems. *Eur J Oper Res* 37:42–57
- Estoque RC, Murayama Y (2013) Landscape pattern and ecosystem service value changes: implications for environmental sustainability planning for the rapidly urbanizing summer capital of the Philippines. *Landscape Urban Plan* 116:60–72
- Estoque RC, Murayama Y (2014) A geospatial approach for detecting and characterizing non-stationarity of land change patterns and its potential effect on modeling accuracy. *GISci Remote Sens* 51:239–252
- Estoque RC, Murayama Y (2016) Quantifying landscape pattern and ecosystem service value changes in four rapidly urbanizing hill stations of Southeast Asia. *Landscape Ecol* 31:1481–1507
- Estoque RC, Murayama Y, Kamusoko C, Yamashita A (2014) Geospatial analysis of urban landscape patterns in three major cities of Southeast Asia. *Tsukuba Geoenviron Sci* 10:3–10
- Friedman JH (2002) Stochastic gradient boosting. *Comput Stat Data Anal* 38:367–378

- Geoghegan J, Villar SC, Klepeis P, Mendoza PM, Ogneva-Himmelberger Y, Chowdhury RR, Turner BL II, Vance C (2001) Modeling tropical deforestation in the Southern Yucatan peninsular region: comparing survey and satellite data. *Agri Ecosyst Environ* 85:25–46
- Google Earth (2015) Google Earth. Accessed on 2 Nov 2013 from <http://www.earth.google.com>
- Hagen A (2002) Multi-method assessment of map similarity. In: 5th conference on geographic information science, 25–27 Apr 2002, Palma de Mallorca, Spain
- Kamusoko C, Gamba J (2015) Simulating urban growth using a random-forest cellular automata (RF-CA) model. *ISPRS Int J Geo-Inf* 4(2):447–470
- Lambin EF (1997) Modelling and monitoring land-cover change processes in tropical regions. *Prog Phys Geogr* 21:375–393
- Liaw A, Wiener M (2002) Classification and regression by randomForest. *R News* 2:18–22
- Liu Y (2009) Modelling urban development with geographical information systems and cellular automata. CRC Press, Taylor & Francis Group, Boca Raton
- Mas JF, Puig H, Palacio J, Sosa-Lopez C (2004) Modelling deforestation using GIS and artificial neural networks. *Environ Model Softw* 19:461–471
- Mas J, Soares-Filho B, Pontius R, Farfan Gutierrez M, Rodrigues H (2013) A suite of tools for ROC analysis of spatial models. *ISPRS Int J Geo-Inf* 2:869–887
- Matheussen B, Kirschbaum RL, Goodman IA, O'Dennel GM, Lettenmaier DP (2000) Effects of land cover change on streamflow in the interior Columbia river basin (USA and Canada). *Hydrol Process* 14(5):867–885
- McGarigal K, Cushman SA, Ene E (2012) FRAGSTATS v4: spatial pattern analysis program for categorical and continuous maps. Computer software program produced by the authors at the University of Massachusetts Amherst. Accessed 1 July 2015 from <http://www.umass.edu/landeco/research/fragstats/fragstats.html>
- Messina J, Walsh S (2001) 2.5D morphogenesis: modeling landuse and landcover dynamics in the Ecuadorian Amazon. *Plant Ecol* 156:75–88
- NASA (2013) Landsat 8 overview. Accessed on 25 May 2013 from [http://www.nasa.gov/mission\\_pages/landsat/overview/index.html](http://www.nasa.gov/mission_pages/landsat/overview/index.html)
- Pontius RG Jr (2002) Statistical methods to partition effects of quantity and location during comparison of categorical maps at multiple resolutions. *Photogram Eng Remote Sens* 68:1041–1049
- Pontius RG Jr, Malanson J (2005) Comparison of the structure and accuracy of two land change models. *Int J Geogr Inf Sci* 19:243–265
- Pontius RG Jr, Parmentier B (2014) Recommendations for using the relative operating characteristic (ROC). *Landscape Ecol* 29:367–382
- Pontius RG Jr, Si K (2014) The total operating characteristic to measure diagnostic ability for multiple thresholds. *Int J Geogr Inf Sci* 28:570–583
- Pontius RG Jr, Walker R, Yao-Kumah R, Arima E, Aldrich S, Caldas M, Vergara D (2007) Accuracy assessment for a simulation model of Amazonian deforestation. *Ann Assoc Am Geogr* 97:677–695
- Pontius RG Jr, Boersma W, Castella JC, Clarke K, de Nijs T, Dietzel C, Duan Z, Fotsing E, Goldstein N, Kok K, Koomen E, Lippit CD, McConnel W, Sood AM, Pijanowski B, Pithadia S, Sweeney S, Trung TN, Veldkamp AT, Verbug PH (2008) Comparing the input, output, and validation maps for several models of land change. *Ann Reg Sci* 42:11–37
- R Development Core Team (2005) R: a language and environment for statistical computing. R Found Stat Comput. Accessed on 3 Apr 2014 from [http://r-prject.kr/sites/default/files/2%EA%B0%95%EA%B0%95%EC%A2%8C%EC%86%8C%EA%B0%9C\\_%EC%8B%A0%EC%A2%85%ED%99%94.pdf](http://r-prject.kr/sites/default/files/2%EA%B0%95%EA%B0%95%EC%A2%8C%EC%86%8C%EA%B0%9C_%EC%8B%A0%EC%A2%85%ED%99%94.pdf)
- Ridgeway G (2006) Generalized boosted regression models. Documentation on the R package “gmb”, version 1.5.7. Accessed on 3 Apr 2014 from <http://www.i-pensieri.com/gregr/gmb.shtml>
- Rodriguez-Galiano VF, Chica-Olmo M, Abarca-Hernandez F, Atkinson PM, Jeganathan C (2012) Random forest classification of Mediterranean land cover using multi-seasonal imagery and multi-seasonal texture. *Remote Sens Environ* 121:93–107

- Soares-Filho BS, Cerqueira GC, Pennachin CL (2002) Modeling the spatial transition probabilities of landscape dynamics in an Amazonian colonization frontier. *BioScience* 51:1059–1067
- Soares-Filho BS, Rodrigues HO, Costa WLS (2009) Modeling environmental dynamics with Dinamica EGO. Accessed on 3 Aug 2009 from <http://www.csr.ufmg.br/dinamica/>
- The State of Land Change Modeling (2014) Advancing land change modeling: opportunities and research requirements. The National Academies Press, Washington, DC
- Tobler W (1979) Cellular geography. In: Gale S, Olsson G (eds) *Philosophy in geography*. Reidel, Dordrecht, pp 379–386
- Torrens PM (2008) Simulating sprawl. *Ann Assoc Am Geogr* 96:248–275
- Townsend PA, Lookingbill TR, Kingdon CC, Gardner RH (2009) Spatial pattern analysis for monitoring protected areas. *Remote Sens Environ* 113:1410–1420
- USGS (2013) Landsat 8 data product information. Accessed on 25 May 2013 from [http://landsat.usgs.gov/LDCM\\_DataProduct.php](http://landsat.usgs.gov/LDCM_DataProduct.php)
- Verburg PH, Veldkamp A, Koning GHJ, Kok K, Bouma J (1999) A spatial explicit allocation procedure for modelling the pattern of land use change based upon actual land use. *Ecol Model* 116:45–61
- Verburg PH, Schot PP, Dijst MJ, Veldkamp A (2004) Land use change modelling: current practice and research priorities. *Geo J* 61:309–324
- Visser H, de Nijs T (2006) The map comparison kit. *Environ Model Softw* 21:346–358
- Vliet J, Bregt AK, Hagen-Zanker A (2011) Revisiting Kappa to account for change in the accuracy assessment of land-use change models. *Ecol Model* 222:1367–1375
- Wolfram S (1984) Cellular automata as models of complexity. *Nature* 311:419–424
- Wu F, Webster CJ (1998) Simulation of land development through the integration of cellular automata and multicriteria evaluation. *Environ Plan B* 25:103–126
- Yeh AGO, Li X (2009) Cellular automata and GIS for urban planning. In: Madden M (ed) *Manual of geographic information systems*. American Society for Photogrammetry and Remote Sensing, Bethesda, MD, USA, pp 591–619

Urban Development in Asia and Africa

Geospatial Analysis of Metropolises

Murayama, Y.; Kamusoko, C.; Yamashita, A.; Estoque,  
R.C. (Eds.)

2017, X, 424 p. 206 illus., 185 illus. in color., Hardcover

ISBN: 978-981-10-3240-0